Linking process and metabolic modelling for the estimation of carbon flux distribution in *Corynebacterium glutamicum* growth in spent sulfite liquor ⋆

Pedro A. Lira-Parada [*] **Peter Sinner** [***] **Michael Kohlstedt** [**] **Julian Kager** [***] **Christoph Wittmann** [**] **Christoph Herwig** [***] **Nadav Bar*** [*]

[*] *Department of Chemical Engineering, Norwegian University of Science and Technology, N-7491 Trondheim*
[**] *Institute of Systems Biotechnology, Saarland University Campus A1.5, 66123 Saarbrucken*
[***] *Institute of Chemical, Environmental and Bioscience Engineering, Technische Universität Wien, Gumpendorfer Straße 1a, 1060 Vienna*

Abstract: Process monitoring in microbial cultures became feasible thanks to the development of accurate measurement devices, including *in-situ* probes to monitor biomass growth, oxygen, carbon dioxide and sugar consumption. In comparison, estimating the metabolic fluxes of the cell factories still rely on analysis based on an under-determined set of equations, and requires an expensive and time consuming methods of verification. This problem intensifies in the presence of complex substrates, in which different sugars are utilized in parallel by the cell factories. In the present study, a growth experiment of *Corynebacterium glutamicum* in spent sulfite liquor was studied. The bioprocess was monitored during batch and fed-batch phases, and a parameter estimation routine was conducted to define a process model and the corresponding uptake rates. A tracking optimization algorithm minimized the error between the measured process fluxes and the equivalent fluxes of the elementary flux modes. The results indicate that the optimization technique obtained a set of elementary modes that are closer to reality than the computed from the metabolic analysis. Taken together, we show that an online estimation of metabolic flux distribution of *C. glutamicum* based on a set of process measurement signals was possible with an optimization function that links the process and metabolic model. The procedure can be complementary to the sophisticated and expensive ^{13}C NMR experimental analytical technique.

Keywords: Bioprocess control, microbial culture, soft sensors, parameter estimation, optimization, model identification

1. INTRODUCTION

Genetic-metabolic networks define the theoretical boundaries of the microbial cell factory, predict key aspects of network functionality, robustness, gene regulation (Stelling et al., 2002). The elementary flux modes (EFM) analysis is a useful tool to characterize cellular metabolism and cellular physiological states with the least amount of experimental data (Trinh et al., 2009), and it represents the simplest metabolic pathways that connect substrate with end-products (Stelling et al., 2002). The main challenge of the EFM is that it contains all feasible steady-state flux vectors of a given metabolic network whether it is biologically relevant or not (Klamt et al., 2017), and therefore the method provides a larger solution space than the one that is relevant to a particular cellular state.

Combined experimental and *in silico* metabolic network studies of *C. glutamicum* have been conducted on glucose, fructose (Kiefer et al., 2004) and sucrose for the production of lysine (Vallino and Stephanopoulos, 1993), 1,5-diaminopentane (Buschke et al., 2013), as well as methods for *in vivo* GC-MS analysis of intracellular amino acids(Wittmann et al., 2002). However, studies with industrial mixture of sugars have not been considered due to its inherent complexity. Procedures to minimize the difference between measured uptake rates with their corresponding rates in the EFM have been presented using a minimization algorithm of the weighted root mean squared error (RMSE) (Soons et al., 2010), but the implementation was only conducted in steady state, whereas microbial cultures change dynamically. In this study, growth experiments in spent sulphite liquor (SSL) of *C. glutamicum* strain were investigated in a fed-batch reactor, where the SSL source is from Borregaard a commercial plant in Sarpsborg, Norway.

⋆ The authors would like to thank Dr. Judith Becker, Fabienne Rössler, Andrea Tuveri and Dr. Gerd Seibold for discussions. This research work has received funding from the Department of Chemical Engineering at NTNU, grant number 70441143, and from the Bio Based Industries Joint Undertaking under the European Union's Horizon 2020 research and innovation program under grant agreement No 790507.

The stoichiometric matrix and the metabolic network were constructed considering the assimilation pathways of SSL. The elementary flux modes were obtained using the *efmtool* (Terzer and Stelling, 2008). The process and metabolic models were linked through a tracking optimization routine to define the temporal active set of elementary flux modes throughout the culture. We test our optimization method with culture fed industrial mixture of sugars that have not been considered due to its inherent complexity.

2. MATERIALS AND METHODS

C. glutamicum ATCC13032 (pVWEx1-manA)(pEKEx3-xylAB) was used in this study, and precultures were prepared as outlined in (Sinner et al., 2020). For growth experiments the bacteria were plated out from glycerol stocks on 2TY agar plates and incubated at 30 °C. Thereby obtained single colonies were then used to inoculate 5 mL precultures (2TY medium) (Sambrook et al., 2001) in glass reaction tubes and incubated at 30°C and 250 rpm for 12 h before they were transferred to 1 L shake flasks containing 100 mL CGXII minimial medium (Eikmanns et al., 1991) with 10 g L^{-1} glucose and 0.5 mM IPTG for another 12 h. The bacteria were separated from the broth by centrifugation at (4000 g, 10 min), and used for the inoculation in the bioreactor to reach an initial optical density at 600 nm of one. Labfors 5 (Infors, Switzerland) were used with a 5 L max working volume. The initial working volume was 3.0 L. The bioreactor batch had an initial optical density of unity, the medium contained CGXII medium (without urea and MOPS), supplemented with 5 % v/v ultrafiltrated SSL (UF-SSL) as carbon source, 50 μg mL^{-1} kanamycin sulfate and 100 μg mL^{-1} spectinomycin dihydrochloride and 1 mM IPTG. Temperature was kept at 30 °C and culture pH was controlled at 6.5 by addition of 6 M ammonium hydroxide and 1 M phosphoric acid. Dissolved oxygen was controlled above 30 % by a cascaded adaption of stirrer speed (400 to 1200 rpm), gassing rate (0.5 to 2 vvm) and oxygen concentration (20.95 to 60 % (v/v)) by supplementing pressurized air with pure oxygen. Fed-batch phase was initiated upon substrate depletion indicated by a drop in CO_2 off-gas concentration (see Section 2.1) below 0.25 %. UF-SSL, supplemented with 1 mM IPTG, was used for feeding with specific growth rate setpoints in the range of 0.01 to 0.12 h^{-1}. All sensor data were stored and managed by Lucullus (Securecell, Switzerland).

2.1 Measurements

The biomass specific rates were calculated under usage of a simple material balance equation for the corresponding component. The best constant reaction rate between two measurement points were determined by Nelder Mead optimization (MATLAB 2020a: fmin). To determine the uncertainty, rate calculations were repeated 500 times by a Gaussian sampling procedure from the measurement uncertainties. CO_2 and O_2 concentrations in the off-gas were measured by infrared and zirconium dioxide sensor modules in a BlueInOne Ferm gas analyzer (BlueSens GmbH, Germany). During the experiment, carbon evolution (CER) and oxygen uptake (OUR) rates were determined with the inflow and outflow concentration differences. Biomass dry cell weight was determined gravimetrically by centrifuging 1.8 mL culture broth at 10000 rpm for 10 min at 4 °C, washing the biomass pellet with phosphate buffered saline and drying the washed pellet in pre-weighed sample tubes at 105 °C for 72 h. Sugars were measured from a filtrated sample by a HPLC procedure implemented on a Thermo Scientific Ulti Mate 3000 with a VA 300/7.8 NUCLEOGEL® Sugar Pb column. The mobile phase was deionized water with a flow rate of 0.4 mL min^{-1} HPLC, and at a temperature 80 °C. The refractive index (RI) detector Shodex RI-101 monitored the signals.

Matlab (Mathworks Inc.) was used for simulations, model fitting and to solve the nonlinear least squares problem that minimized the difference between the experimental flux data and the data obtained from the elementary flux matrix. For this we computed the euclidean difference between the experimental data and the *in-silico* EFM data (Schuetz et al., 2007). The *efmtool* was used to obtain the EFM (Terzer and Stelling, 2008). Integration needed for simulations and the sensitivity analysis was conducted with Runge Kutta algorithm *ode45*.

3. RESULTS

3.1 Bioreactor procedure

Microbial systems consists of a vector of $\mathbf{x}$ states, $\mathbf{u}$ inputs, $\mathbf{p}$ parameters, time t and observations $\mathbf{y}$, with the following general non-linear form:

$$\dot{\mathbf{x}}(t) = \mathbf{f}(\mathbf{x}(t), \mathbf{u}(t), \mathbf{p}) \tag{1}$$

$$\mathbf{y}(t) = \mathbf{g}(\mathbf{x}(t), \mathbf{p}) \tag{2}$$

During the experiments, the concentration of sugars and biomass were measured, and the uptake rates could be estimated. The general bioreactor mass balances are:

$$\begin{aligned} \dot{V} &= F_{in} - F_{out}, & \dot{X} &= -\frac{XF_{in}}{V} + \mu X \\ \dot{\mathbf{s}} &= (\mathbf{s_{in}} - \mathbf{s})\frac{F_{in}}{V} - \mathbf{q_s}X, & \dot{\mathbf{P}} &= -\frac{\mathbf{P}F_{in}}{V} + \mathbf{q_P}X \\ \mathbf{c}\dot{X} &= \mathbf{c}\dot{X} + X\dot{\mathbf{c}} = (\mathbf{N}\cdot\mathbf{q})X \end{aligned} \tag{3}$$

Where the model states are the volume (V), biomass (X), a vector of substrate ($\mathbf{s}$), products ($\mathbf{P}$), and internal metabolites ($\mathbf{c}$). The system has an inlet flow (F_{in}), with a sugar concentration ($\mathbf{s_{in}}$), an outlet flow (F_{out}), the specific growth rate (μ), a vector of specific substrate uptake rates ($\mathbf{q_s}$), intracellular specific flux ($\mathbf{q}$) the specific product formation ($\mathbf{q_p}$), and the stoichiometric matrix ($\mathbf{N}$) with m metabolites in r reactions. A summary of uptake rates considered in this study are in Table 1 (Sinner et al., 2019, 2020), and the model parameters are in Table 2.

The total sugar uptake rate (q_{SSL}) takes into consideration the SSL mol composition, where ($MM_{glc}, MM_{xyl}, MM_{Man}$) corresponds to the molar mass of glucose, xylose and mannose, respectively, and the molecular weight of *C. glutamicum* is $MM_{C.glutamicum} = 107.5$ $gmol^{-1}$ (Vallino and Stephanopoulos, 1993). We took into account the previous sugars because this genetically modified strain is capable of metabolizing them. Since we link the process model to the metabolic model, the process model sugar uptake

Table 1. Summary of uptake rates

Uptake rates
$q_{Glc} = q_{S_1} = q_{mS_1}\left(\frac{S_1}{K_{S_1}+S_1}\right),$
$q_{Xyl} = q_{S_2} = q_{mS_2}\left(\frac{S_2}{S_2+\frac{K_{S_2}}{K_{S_1}}S_1+\frac{K_{S_2}}{K_{S_3}}S_3+K_{S_2}}\right)$
$q_{Man} = q_{S_3} = q_{mS_3}\left(\frac{S_3}{S_3+\frac{K_{S_3}}{K_{S_1}}S_1+\frac{K_{S_2}}{K_{S_1}}S_2+K_{S_3}}\right)$
$OUR = \frac{XV}{DOR_{O_2}}\sum_i q_{S_i}\left(\frac{DOR_{S_i}}{M_{C-molSi}} - \frac{Y_{XS_i}}{M_{C-molX}}\right)$
$CER = XV\sum_i q_{S_i}\left(\frac{1}{M_{C-molSi}} - \frac{Y_{XS_i}}{M_{C-molX}}\right)$
$\mu = \sum_i q_{S_i} Y_{XS_i}$
$q_{SSL} = \frac{q_{S1}}{4.9\cdot10^{-2}\cdot MM_{Glc}} + \frac{q_{S2}}{8.1\cdot10^{-2}\cdot MM_{xyl}} + \frac{q_{S3}}{1.54\cdot10^{-1}\cdot MM_{Man}}$

rates were normalized with respect to the SSL uptake rate, a common procedure metabolic model computations, for instance:

$$q^{SSL}_{glc} = \frac{q_{Glc}}{q_{SSL}}, \quad q^{SSL}_{\mu} = \frac{\mu}{q_{SSL}\cdot MM_{Cglutamicum}}$$
$$q^{SSL}_{OUR} = \frac{OUR}{X\cdot V\cdot q_{SSL}}, \quad q^{SSL}_{CER} = \frac{CER}{X\cdot V\cdot q_{SSL}} \qquad (4)$$

Table 2. Process model parameters.

Parameter	Value	Unit	Uncertainty
q_{Glc}	0.176	$g\cdot g^{-1}\cdot h^{-1}$	±0.27%
q_{Xyl}	0.11804	$g\cdot g^{-1}\cdot h^{-1}$	±1.3%
q_{Man}	0.20558	$g\cdot g^{-1}\cdot h^{-1}$	±1.2%
K_{Glc}	0.0017	$g\cdot L^{-1}$	±12.9%
K_{Xyl}	1.1167	$g\cdot L^{-1}$	±2.15%
K_{Man}	0.92684	$g\cdot L^{-1}$	±1.7%
Y_{XS_1}	0.55984	$g\cdot g^{-1}$	±1.7%
Y_{XS_2}	0.32163	$g\cdot g^{-1}$	±4.1%
Y_{XS_3}	0.42737	$g\cdot g^{-1}$	±4.6%
S_{Glc-in}	46.07	$g\cdot L^{-1}$	±25%
S_{Xyl-in}	126.35	$g\cdot L^{-1}$	±25%
S_{Man-in}	69.98	$g\cdot L^{-1}$	±25%
$M_{Cmol-S_{1,2,3}}$	30.03	$[g\cdot Cmol^{-1}]$	–
M_{Cmol-X}	27.28	$[g\cdot Cmol^{-1}]$	–
DOR_{O_2}	-4	$[mol_{e^-}\cdot Cmol^{-1}]$	–
$DOR_{S_{1,2,3}}$	4	$[mol_{e^-}\cdot Cmol^{-1}]$	–
DOR_X	4.18	$[mol_{e^-}\cdot Cmol^{-1}]$	–

Figure 1 presents the results of the experimental fed-batch *C. glutamicum* culture (in black dots, and gray confidence area), and the results of the process model after parameter estimation (blue lines, blue area). The process has a non-linear behaviour of biomass growth and sugar consumption in SSL as a function of time. The CDW values increased during the batch phase followed by a short steady state in the biomass when sugar were depleted (time 25-35 hr). The subsequent fed-batch phase of the process further increased the biomass concentration. An exponential substrate feeding started when the CO_2 concentration was below 0.25%, and the SSL inlet feeding triggered a new growth phase. The OUR and CER signals increased during the batch and the feeding phases, exhibiting typical fed-batch process dynamics (Paczia et al., 2012). During the batch phase, glucose, xylose and mannose were consumed consecutively, as discussed in previous publications (Sinner et al., 2020, 2019). Microbial growth rate was found to be highly variable during the process (black dashed in Figure 2 calculated from the experiments, blue dashed from model simulations), and was highest during high glucose concentrations. Uptake rates of xylose and mannose (expressed

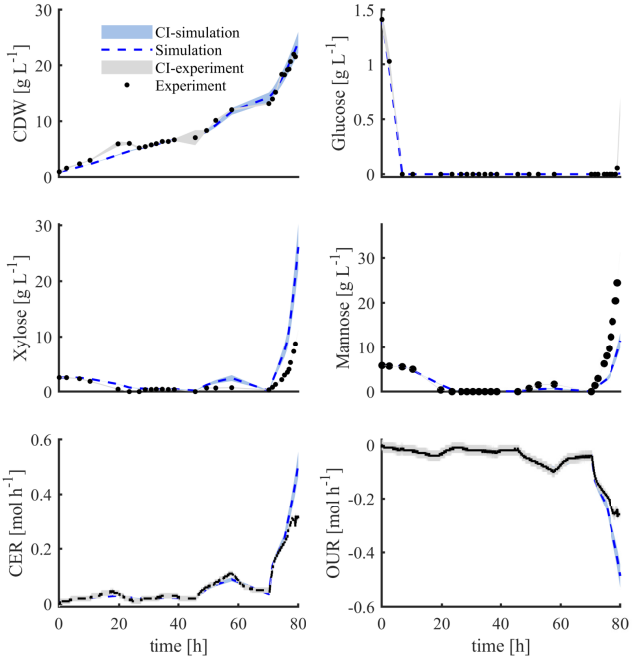

Fig. 1. Fed-batch experimental data of cell dry weight (CDW), sugars concentrations, oxygen uptake rate (OUR) and carbon evolution rate (CER). The black circles correspond to the measured values with confident intervals (CI) in gray area. The simulations with the model are represented with blue dashed lines, and the CI of the model with a blue area.

by grams sugars per gram SSL per hour) were highly variable during the process, with mannose exhibiting its high uptake rate following glucose depletion.

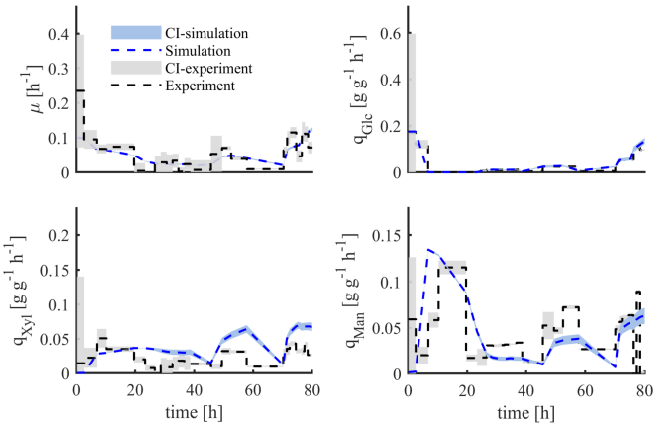

Fig. 2. Microbial growth rate (μ) and specific uptake rates as a function of time.

When the uptake rates of the different sugars were normalized with the rate of the SSL (q_{SSL}) and computed the confident intervals (CI) of these ratios (Figure 3), it was found that the CI were largest in the start of the batch phase when the biomass is lowest (due to large CDW measurement error) but also when the individual sugars were depleted (glucose, mannose and xylose). Moreover, xylose exhibits large CI regions during most of the process, implies uncertainty in the uptake calculations of xylose. Due to this high uncertainty from the measurements, we

propose in this study to use the process model to estimate the normalized uptake rates.

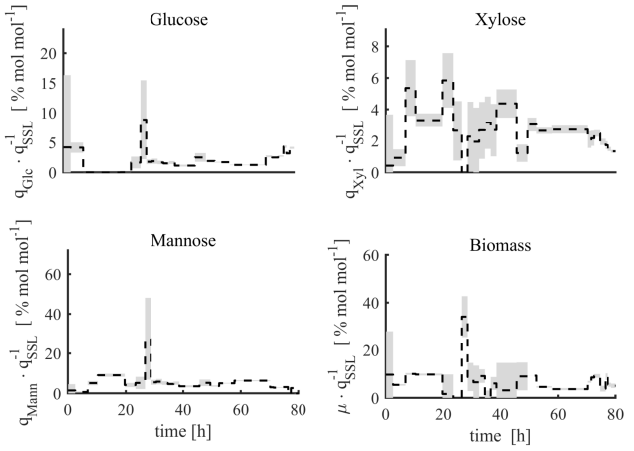

Fig. 3. Experimental normalized uptake rates as a function of time during the process. The dashed lines represent the value of the relative fluxes, and the gray area correspond to the confidence intervals.

3.2 Elementary flux mode analysis

Metabolic steady state implies constant metabolite concentrations as a function of time ($\dot{\mathbf{c}} = 0$), and the quasi-steady state (QSS) of the internal metabolites is (Ben Yahia et al., 2017):

$$\dot{\mathbf{c}} \approx \mathbf{0} \Rightarrow 0 = \mathbf{N} \cdot \mathbf{q} + (\frac{F_{in}}{V} - \mu)\mathbf{c}$$
$$(\mu - \frac{F_{in}}{V})\mathbf{c} = \mathbf{N} \cdot \mathbf{q} \quad (5)$$

Assuming, the order of magnitude of cell growth and dilution are smaller than the flux contribution, Equation 5 becomes (Zupke and Stephanopoulos, 1995):

$$\mathbf{0} = \mathbf{N} \cdot \mathbf{q} \quad (6)$$

where $\mathbf{N} \in \mathbb{R}^{mxr}$ where m is the number of metabolites, and r are the number of reactions, and the vector of rates is $\mathbf{q} \in \mathbb{R}^{rx1}$. The solution of Equation 6 corresponds to the admissible flux space which form the unique convex basis of the polyhedral cone (Rockafellar, 1970). The nonzero vectors of the flux cone are the EFM. The EFM are defined by a set of vectors $\mathbf{q}$ that describes the net flux rate of the corresponding reaction. The convex polyhedral cone is denoted as the flux cone (FC) of flux vectors that satisfy Equation 6, with some irreversibility reaction constraints (Irr) (Klamt et al., 2017; Gagneur and Klamt, 2004):

$$FC = \{\mathbf{q} \in \mathbb{R}^n \mid \mathbf{N} \cdot \mathbf{q} = \mathbf{0}, q_i \geq 0 \text{ for } i \in Irr\} \quad (7)$$

The matrix of EFMs ($\mathbf{E} = q_{r,k}$) has r reactions (rows) and k elementary modes (columns):

$$\mathbf{E} = [\mathbf{q_1},\ \mathbf{q_2},\ ...,\ \mathbf{q_k}] \quad (8)$$

Firstly, we proceed with the metabolic representation of the metabolic network (Wittmann and Lee, 2012). Secondly, the stoichiometric matrix $\mathbf{N}$ was defined, and the EFM matrix was calculated solving Equation 6 (Orth et al., 2010) with the *efmtool* (Terzer and Stelling, 2008). Table 3 presents the number of metabolites, reactions, stoichiometry, and the EFM size.

Table 3. EFM analysis

Metabolites	53	Stoichiometry	53x63
Reactions	63	Number of EFMs	63x18901

The EFM matrix $\mathbf{E}$ presents all the potential rates that can be obtained from the metabolic model (Table 3), although these rates are not necessarily active during the actual process. The metabolic model is static, describing all the possible reaction that can occur, whereas at any given time during the process some reactions can be active and others inactive (representing zero flux through the reaction). In our case study, it implies that the matrix $\mathbf{E}$ in Equation 8 is a matrix that contains 63 reactions (rows) and all the possible combinations (modes, in columns), each representing a solution, i.e. potential uptake rate vector. Because the number of solution can be large (Table 3 presents 18901 solutions), the aim is to develop an algorithm that can narrow down the number of solutions to relevant ones during a given time. Figures 4 a-c represent several two dimensional projections of the uptake rates that were calculated by the EFM algorithm and obnained by the corresponding r-reactions (rows) and k-modes (columns) of the matrix E (black dots). The projections include product formation as a function of biomass production from SSL (Figure 4a), O_2 consumption as a function of CO_2 production from SSL (Figure 4b), and the biomass formation as a function of CO_2 from SSL (Figure 4c). In each projection, these calculated rates define the theoretical span of the possible (feasible) values that these rates can be in the microbial cell factory. Interestingly, when plotting the same rate projections of the q_i values from the process model (red dots), we find that they are located within the same regions of the theoretical EFM from the corresponding rows of matrix $\mathbf{E}$ (black dots), which serves as a validation. Firstly, since the cell factories are not producing the product (peptide), the process model data (red dots) lie on the $q_{pep} = 0$ axis (Figure 4a). The O_2 consumption and CO_2 production follow a linear relationship, for both, the EFM results and the process model equation, and that the stoichiometric model and the process model are in agreement with respect to linearity in the respiratory coefficient (RQ = $\frac{CO_2 - produced}{O_2 - consumed}$). Finally, biomass formation as a function of CO_2 production is constrained and defined in a region. Hence, consistency between the result of the complete elementary flux matrix and the process model was observed in the phase plot diagrams.

3.3 Optimization Procedure

As was mentioned before, the aim is to develop an optimization algorithm that confine the number of solutions to the most relevant ones at any given time during the process. The optimization procedure minimizes the difference between the output of the reaction (r) relative uptake rate from the elementary flux matrix $\mathbf{E}$ (Equation 8), and the r-relative uptake rates estimated from the process model.

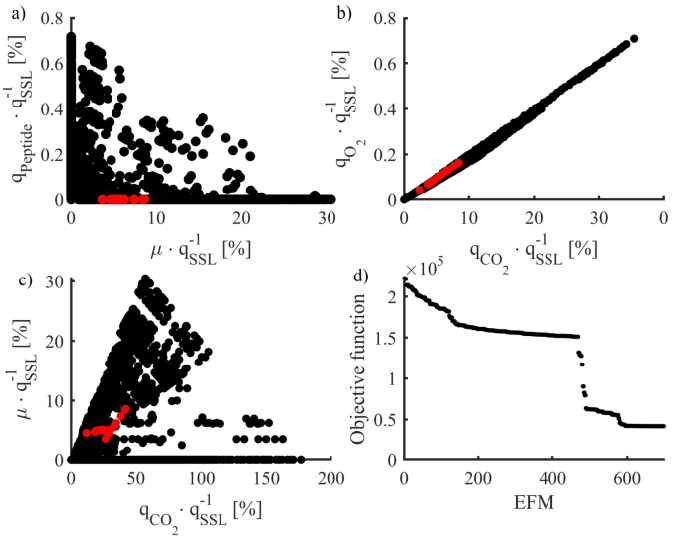

Fig. 4. Phase plot diagrams (a-c) from the EFM (black dots), and model simulation (red dots). d) Objective function as a function of EFM.

The optimization problem computes at each time T the closest modes from the EFM matrix $\mathbf{E}$ that minimize:

$$\min_{k\in\mathbb{R}^{n_k}} J_{KT} = \sum_r \frac{(\mathbf{q}^{SSL}_{r_{process}} - \mathbf{q}^{SSL}_{k,r_{EFM}})^2}{max(\mathbf{q}^{SSL}_{r_{process}})} \quad \text{s.t. } \mathbf{N}\cdot\mathbf{q} = \mathbf{0} \tag{9}$$

where the k modes from the $\mathbf{E}$ matrix ($\mathbf{q}^{SSL}_{k,r_{EFM}}$) and their r-reaction equivalent from the process model ($\mathbf{q}^{SSL}_{r_{process}}$). Figure 4d presents the euclidean difference between process model and different modes in the EFM matrix. Then, a selection of (n_L) modes that have the lowest numerical value in Equation 9 is done, and an average value (q_{av-L}) of the reactions with the modes selected:

$$q_{av-L} = \sum_L \frac{q^{SSL}_{k,r_{EFM}}}{n_L} \tag{10}$$

The EFM matrix and the process model were linked through the optimization algorithm. Figure 5 presents the uptake ratio of glucose, xylose, mannose, O_2 and production of biomass and CO_2. The computed optimized solution (green lines) is the average of the closest modes obtained from the optimization procedure with Equation 9. The results follow the process model (blue line), and the normalized fluxes computed by the optimization problem follow the rates obtained from the experiments.

The non-redundancy in the stoichiometric matrix can be evaluated through the pseudo inverse of the stoichiometric matrix. For that, a metabolic flux analysis (MFA) and a multiple linear regression (MLR) were conducted, but a non-unique solution was found for the MFA and the result presented not finite confidence intervals in the MLR.

The resulting r reaction rates from the optimization problem as functions of the process time can be represented as a heat map (Figure 6). The data was normalized with respect to their own maximum in the process allowing to compare the simulation through the microbial culture. The heat map derives information on the dynamics of the cellular and metabolic activities of the cell factories during the bioprocess. This information is not obtained by the static

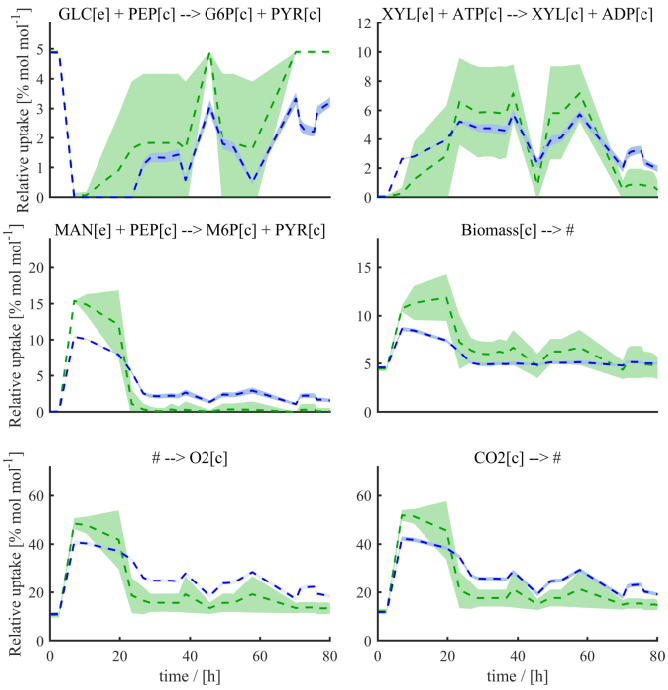

Fig. 5. Ratio of uptake rates. The results show in blue lines the model simulation and in blue area the confidence interval for the simulation. The green line corresponds to the average from the solution of the optimization problem from the EFM selection, and the green area is the standard deviation of the selected modes.

metabolic flux analysis (Eq. 6). Most importantly, the well stablished ^{13}C methods to obtain temporal metabolic states from experiments require a defined medium, deriving experimental data, for instance by using of this dynamic on the cellular metabolic state is challenging, and compared to other studies, this study is in a complex mixture of sugars, and it is a limitation for the ^{13}C method.

4. CONCLUSIONS

The estimation of the relative uptake rates throughout a culture was conducted using a process model and an tracking optimization function. The objective function minimized the difference between process and the matrix of the elementary flux analysis, and it estimated the flux distribution in the bioreactor, the proposed procedure can be complemented with dedicated ^{13}C experiment when required.

REFERENCES

Bassem Ben Yahia, Boris Gourevitch, Laetitia Malphettes, and Elmar Heinzle. Segmented linear modeling of CHO fed-batch culture and its application to large scale production. *Biotechnology and Bioengineering*, 114(4): 785–797, 2017. doi: 10.1002/bit.26214.

Nele Buschke, Judith Becker, Rudolf Schäfer, Patrick Kiefer, Rebekka Biedendieck, and Christoph Wittmann. Systems metabolic engineering of xylose-utilizing *Corynebacterium glutamicum* for production of 1,5-diaminopentane. *Biotechnology Journal*, 8(5):557–570, 2013. doi: 10.1002/biot.201200367.

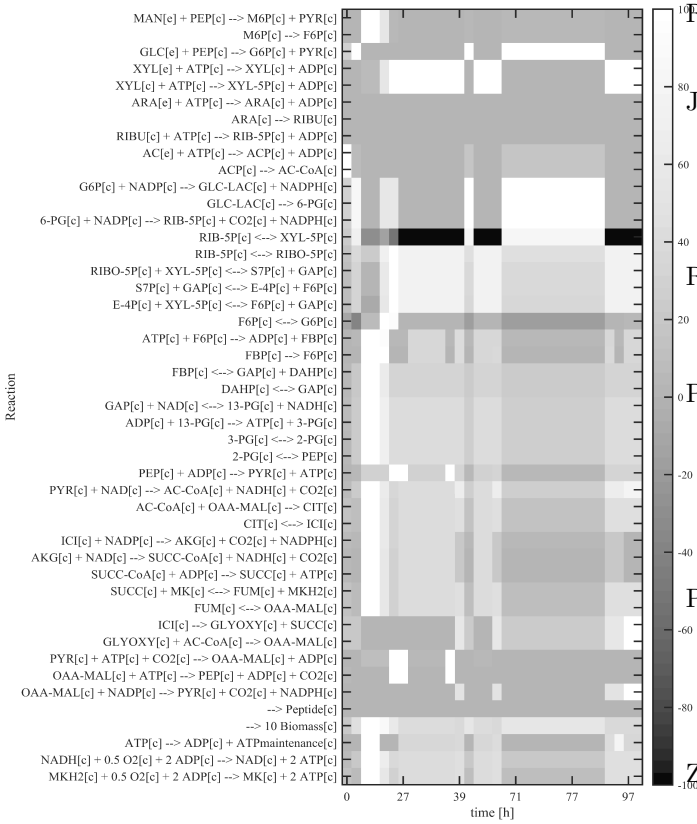

Fig. 6. Normalized activity of each reaction as a function of time.

BJ Eikmanns, M Metzger, D Reinscheid, M Kircher, and H Sahm. Amplification of three threonine biosynthesis genes in *Corynebacterium glutamicum* and its influence on carbon flux in different strains. *Applied Microbiology and Biotechnology*, 34(5):617—622, February 1991. ISSN 0175-7598. doi: 10.1007/bf00167910.

Julien Gagneur and Steffen Klamt. Computation of elementary modes: a unifying framework and the new binary approach. *BMC Bioinformatics*, 5(1):175, 2004. doi: 10.1186/1471-2105-5-175.

Patrick Kiefer, Elmar Heinzle, Oskar Zelder, and Christoph Wittmann. Comparative metabolic flux analysis of lysine-producing *Corynebacterium glutamicum* cultured on glucose or fructose. *Applied and Environmental Microbiology*, 70(1):229–239, 2004. ISSN 0099-2240. doi: 10.1128/AEM.70.1.229-239.2004.

Steffen Klamt, Georg Regensburger, Matthias P Gerstl, Christian Jungreuthmayer, Stefan Schuster, Radhakrishnan Mahadevan, Jürgen Zanghellini, and Stefan Müller. From elementary flux modes to elementary flux vectors: Metabolic pathway analysis with arbitrary linear flux constraints. *PLoS Computational Biology*, 13 (4), 2017. doi: 10.1371/journal.pcbi.1005409.

Jeffrey D Orth, Ines Thiele, and Bernhard Ø Palsson. What is flux balance analysis? *Nature biotechnology*, 28(3):245–248, 2010. doi: 10.1038/nbt.1614.

Nicole Paczia, Anke Nilgen, Tobias Lehmann, Jochem Gätgens, Wolfgang Wiechert, and Stephan Noack. Extensive exometabolome analysis reveals extended overflow metabolism in various microorganisms. *Microbial Cell Factories*, 11(1):122, 2012. doi: 10.1186/1475-2859-11-122.

R Tyrrell Rockafellar. *Convex analysis*. Number 28 in Princeton Mathematical Series. Princeton University Press, Princeton, N. J., 1970.

J. Sambrook, D.W. Russell, C.A. Irwin, Cold Spring Harbor Laboratory, Ralph Erskine Conrad Memorial Fund, and K.A. Janssen. *Molecular Cloning: A Laboratory Manual*. Number V. 1 in Molecular Cloning: A Laboratory Manual. Cold Spring Harbor Laboratory Press, 2001. ISBN 9780879695767.

Robert Schuetz, Lars Kuepfer, and Uwe Sauer. Systematic evaluation of objective functions for predicting intracellular fluxes in escherichia coli. *Molecular Systems Biology*, 3(1):119, 2007. doi: 10.1038/msb4100162.

Peter Sinner, Julian Kager, Sven Daume, and Christoph Herwig. Model-based analysis and optimisation of a continuous *Corynebacterium glutamicum* bioprocess utilizing lignocellulosic waste. *IFAC-PapersOnLine*, 52(26):181 – 186, 2019. ISSN 2405-8963. doi: 10.1016/j.ifacol.2019.12.255. 8th Conference on Foundations of Systems Biology in Engineering FOSBE 2019.

Peter Sinner, Marlene Stiegler, Christoph Herwig, and Julian Kager. Noninvasive online monitoring of *Corynebacterium glutamicum* fed-batch bioprocesses subject to spent sulfite liquor raw material uncertainty. *Bioresource Technology*, page e124395, 2020. ISSN 0960-8524. doi: 10.1016/j.biortech.2020.124395.

Zita I.T.A. Soons, Eugénio C. Ferreira, and Isabel Rocha. Selection of elementary modes for bioprocess control. *IFAC Proceedings Volumes*, 43(6):156–161, 2010. ISSN 1474-6670. doi: 10.3182/20100707-3-BE-2012.0019. 11th IFAC Symposium on Computer Applications in Biotechnology.

Jörg Stelling, Steffen Klamt, Katja Bettenbrock, Stefan Schuster, and Ernst Dieter Gilles. Metabolic network structure determines key aspects of functionality and regulation. *Nature*, 420(6912):190–193, 2002. doi: 10.1038/nature01166.

Marco Terzer and Jörg Stelling. Large-scale computation of elementary flux modes with bit pattern trees. *Bioinformatics*, 24(19):2229–2235, 2008. doi: 10.1093/bioinformatics/btn401.

Cong T Trinh, Aaron Wlaschin, and Friedrich Srienc. Elementary mode analysis: a useful metabolic pathway analysis tool for characterizing cellular metabolism. *Applied Microbiology and Biotechnology*, 81(5):813, 2009. doi: 10.1007/s00253-008-1770-1.

Joseph J. Vallino and Gregory Stephanopoulos. Metabolic flux distributions in *Corynebacterium glutamicum* during growth and lysine overproduction. *Biotechnology and Bioengineering*, 41(6):633–646, 1993. doi: 10.1002/bit.260410606.

Christoph Wittmann and Sang Yup Lee. *Systems metabolic engineering*. Springer Science & Business Media, 2012. doi: 10.1007/978-94-007-4534-6.

Christoph Wittmann, Michael Hans, and Elmar Heinzle. In vivo analysis of intracellular amino acid labelings by gc/ms. *Analytical Biochemistry*, 307(2):379–382, 2002. ISSN 0003-2697. doi: 10.1016/S0003-2697(02)00030-1.

Craig Zupke and Gregory Stephanopoulos. Intracellular flux analysis in hybridomas using mass balances and in vitro 13C NMR. *Biotechnology and Bioengineering*, 45 (4):292–303, 1995. doi: 10.1002/bit.260450403.